Spatially Resolved Millimeter Spectroscopy of the Gravitational Lens PKS 1830-211

Jonathan J. Swift & William J. Welch

Radio Astronomy Laboratory, and Department of Astronomy, University of California, Berkeley, CA 94720

Brenda L. Frye

Lawrence Berkeley National Laboratory, Department of Physics, University of California, Berkeley, CA 94720

ABSTRACT

This paper presents data from the BIMA interferometer showing spatially resolved absorption spectra of the gravitationally lensed quasar PKS 1830-211. High-resolution ($1.2\,\mathrm{km\,s^{-1}}$) spectra were taken in two spectral windows centered on the redshifted frequencies of the $HCO^+(2 \leftarrow 1)$ and $HCN(2 \leftarrow 1)$ molecular transitions. There is no molecular absorption in the northeast image but the southwest image reveals optically thick absorbing gas at these transition frequencies. Further analyses conclude that the spectra are consistent with completely saturated absorption in the southwest image and the line profiles suggest that the absorbing medium is complex, perhaps containing multiple components and small scale structure. The absorption occurs along a pencil beam through the lensing galaxy which is thought to be a late type spiral oriented almost face on. However, the spectra show absorption spanning more than $60\,\mathrm{km\,s^{-1}}$ which is difficult to explain for this scenario.

Subject headings: quasars: individual (PKS1830-211) — gravitational lensing — galaxies: ISM — ISM: molecules

1. Introduction

PKS 1830-211 is a radio bright source determined to be a gravitationally lensed quasar from its ring-like morphology (Jauncey et al. 1991; Subrahmanyan et al. 1990; Rao & Subrahmanyan 1988) toward which molecular absorption has been detected (Wiklind & Combes 1996). The object consists of two flat spectrum images connected by a nearly circular, low surface brightness steep spectrum Einstein ring (Jauncey et al. 1991; Kochanek & Narayan 1992). The two bright sources are separated by $\sim 1''$ and lie to the northeast (NE) and southwest (SW) of the ring center.

Wiklind and Combes (1996) discovered twelve different rotational transitions involving five different molecular species toward PKS 1830-211 in unresolved spectra. The lines had widths of

$\sim 30\,\mathrm{km\,s^{-1}}$, depths of $\sim 40\%$, and were redshifted to $z = 0.89$. Based on standard isotopic ratios, the detection of $\mathrm{H^{13}CO^+}(2 \leftarrow 1)$ implied that the $\mathrm{HCO^+}(2 \leftarrow 1)$ was optically thick. This assumption along with published flux ratios of the NE and SW components led to the conclusion that the absorption was only in the southwest component. Spectra of the two main components were obtained with the Berkeley Illinois Maryland Association (BIMA) array by resolving the source in the 3-mm band (Frye et al. 1996). The molecular absorption only appeared in the SW component as was expected, but did not reach the zero flux level. These results seemed to conflict with an analysis done by Wiklind and Combes (1998) on the unresolved spectrum of PKS 1830-211 where the shift in the field phase center at the frequency corresponding to the $\mathrm{HCO^+}(2 \leftarrow 1)$ transition was consistent with saturated absorption in the SW image.

High-resolution $\mathrm{HCO^+}(2 \leftarrow 1)$ spectra of the unresolved source taken with the Plateau de Bure interferometer (Wiklind & Combes 1998) showed that the trough of the absorption is not flat as would be expected from complete saturation. The line profile was also clearly asymmetric with the broader wing toward negative velocities. These results are reasonable for absorption due to a multi-component cloud with possible small scale structure rather than one optically thick cloud.

Galactic models (Wiklind & Combes 1998), a determination of the quasar redshift, $z = 2.5$ (Lidman et al. 1998), and lensing models (Nair et al. 1993; Kochanek & Narayan 1992) combined to form a coherent picture of this gravitational lens system and the Hubble parameter was determined to be $H_0 = 65^{+15}_{-9}\,\mathrm{km\,s^{-1}\,Mpc^{-1}}$ (Lidman et al. 1998). The rather large uncertainty in the time delay measurement, about 20% (Lovell et al. 1998), is the major source of error in this estimate of H_0. Continued monitoring of the flux ratio of PKS 1830-211 would allow for a better estimate of the time delay and therefore a better determination of the Hubble parameter. The flux ratio can be easily determined from an unresolved spectrum of the source if the absorption in the SW image is saturated (Wiklind & Combes 1996). While many lines have been studied in this system, high-resolution spectra of saturated absorption in the resolved SW image have yet to be presented.

This paper presents observations of PKS 1830-211 made with the BIMA interferometer in Hat Creek, California (Welch et al. 1996) which yielded spectra of the two individual components. There have been a couple of important improvements to the BIMA array since the published results of Frye et al. (1996). The most significant upgrade has been the installation of new SIS mixers in 1997 which has halved the receiver noise temperatures (Engargiola & Plambeck 1998). There have also been new A-array stations added which produce a better imaging beam. The observations presented here were done with higher spectral resolution than the previous BIMA observations and were intended to give a more detailed look at the line profile of the resolved SW image. In § 2 the observations and observing conditions are outlined and the details of the self-calibration procedure used in the data reduction are given. Section 3 presents flux values and an analysis of the spectra. Rotation temperatures, column depths, and the implications of the line profiles are then discussed in § 4.

2. Observations and Data Reduction

PKS 1830-211 was observed in the 3-mm band using the "A-" configuration of the BIMA array which is the standard A configuration without the longest baselines at 1.9 km. The correlator was set so that in each sideband there were two spectral windows containing 128 channels with a spectral resolution of $1.2\,\mathrm{km\,s^{-1}}$ and four wide band windows each containing 32 channels and spanning 100 MHz. The first local oscillator was tuned so that the redshifted $(2 \leftarrow 1)$ rotational transitions of HCO^+ and HCN, at 94.588 GHz and 93.977 GHz respectively, fell into the two high resolution windows. The HCO^+ line was Doppler tracked throughout the observations. The standard quasar 3C273 was observed to calibrate the passband, Uranus gave an absolute flux scale, and 1733-130 was used as a secondary calibrator. PKS 1830-211 was observed in 30 minute intervals using 23 second integrations with the intention of self calibration.

Data were used from two separate observing tracks on 1999 December 27 and 28. The observations on the 27th were good with typical system temperatures between 200 K and 300 K and the RMS phase variations measured on 100 m baselines were on the order of $200\,\mu$m. The atmospheric conditions on the 28th were even better with slightly lower system temperatures and phase variations of $\sim 80\,\mu$m.

PKS 1830-211 is a bright source which can be self calibrated on a record-by-record basis. The data on each day was split into two datasets corresponding to the upper and lower side bands and the phases were first corrected in the lower side band using an iterative self-calibration process. The first iteration used a point source at the observing center as a model, and produced a two-component image. The inverted CLEAN model containing two main components was then used as the self-calibration model in the subsequent iteration. Two self-calibration iterations were needed for the image to converge. The upper side band was then phase calibrated in the same way with the only difference being that the first model used in the self-calibration iteration was the CLEAN model from the lower side band. The spectral windows were then phase calibrated channel by channel using a 65 minute time interval allowing enough signal for a reliable calibration. The bandpass was determined from 3C273 and was applied to the source and then the datasets were scaled to the flux of Uranus measured on December 27. The calibrated datasets were then combined and inverted into a single plane upper side band continuum map and two 128 plane spectral cubes. All reductions were done using the MIRIAD software package.

The two main components were not resolved to a sufficient degree in all of the data due to the position angle of the synthesized beam and therefore some data were discarded. A local sidereal time range of 1700–1900 was used on both nights covering an elevation range from 17 to 27°. The resulting synthesized beam dimensions are $1''.08 \times 0''.59$ FWHM with a position angle of $-11.6°$. This resolution issue and the implications will be considered further in the following section.

3. Analysis and Results

The combined datasets yield a NE continuum level of $1.13 \pm 0.1\,\mathrm{Jy\,beam^{-1}}$ and a SW level of $0.96{\pm}0.1\,\mathrm{Jy\,beam^{-1}}$ with the flux levels of the individual datasets agreeing to within 10%. Although this is known to be a highly variable source (van Ommen et al. 1995), these levels are reasonable in comparison to previous results (Wiklind & Combes 1998; Frye et al. 1996; Wiklind & Combes 1996). The flux ratio of the two images, 1.18 ± 0.06, is expected to be more accurate than the overall flux scale and agree to within 3% on the two days. The separation angle was determined using the inverted CLEAN model of the combined datasets giving a value of $0''.99 \pm 0''.05$, consistent with previously published values (Rao & Subrahmanyan 1988; Subrahmanyan et al. 1990; Nair et al. 1993; Johns et al. 1996; Frye et al. 1996).

Spectra were taken from the two 128 plane data cubes containing the $HCO^+(2 \leftarrow 1)$ and $HCN(2 \leftarrow 1)$ transitions at the locations of the continuum peaks (see Fig. 1). The line profiles obtained here are in good qualitative agreement with the high resolution ($0.5\,\mathrm{km\,s^{-1}}$) spectrum of $HCO^+(2 \leftarrow 1)$ in Fig. 7 of Wiklind and Combes, 1998 (hereafter 7WC). The absorption widths are comparable at about $45\,\mathrm{km\,s^{-1}}$ FWHM, and the asymmetry in the lines is apparent with the broader side toward negative velocities. There is some residual flux in the trough of the absorption, however there is no apparent slope as seen in 7WC.

The absorption in the SW image reaches the zero level with 5 channels at or below zero flux in the HCO^+ window and 3 channels in the HCN window. In reference to 7WC, a numerical average over $20\,\mathrm{km\,s^{-1}}$ (16 channels) around the centroid of the lines was computed giving an average flux level in the absorption trough. This procedure applied to the high-resolution profile of $HCO^+(2 \leftarrow 1)$ in 7WC yielded a value of $\sim$ 0.04–0.06 Jy due to the slope of flux in the absorption trough assuming that the negative velocity edge of the the narrow profile corresponds to a zero flux level in the SW image. The NE and SW components are known to have sizes at or below the milliarcsecond scale (Johns et al. 1996), however the two images in our dataset did not deconvolve into two point sources. A no noise, no phase error model of our observations revealed flux contamination between the two images at the level of $0.01\,\mathrm{Jy\,beam^{-1}}$ preventing a double point source deconvolution. Therefore the flux of a saturated line averaged across the narrow trough given the profile of 7WC and our resolution determined from models is expected to be between 0.05–0.07 $\mathrm{Jy\,beam^{-1}}$. The average flux levels measured in the absorption troughs of the present data are 0.058 and 0.066 $\mathrm{Jy\,beam^{-1}}$ for the HCO^+ and HCN lines respectively.

The data show no evidence of absorption in the NE component in HCO^+ however a small absorption feature is noticeable in the HCN window at $0\,\mathrm{km\,s^{-1}}$. This feature appeared only in the December 28 data and is small but statistically significant reaching the 3σ level. It is interpreted as a small amount of contamination from the SW component.

4. Discussion

This dataset is unique in showing direct evidence of spatially and spectrally resolved saturated absorption in PKS 1830-211. The noise in our spectra, with a measured RMS of 0.098 Jy beam^{-1}, is too high to verify the upward slope from negative to positive velocities in the HCO^+ window which is seen in 7WC. However, the absorption does reach zero flux levels in multiple channels in each window and the profile is consistent with saturation given the profile in 7WC and the observational models constructed.

These results are contrary to the results obtained by Frye et al. (1996) who also used the BIMA array to resolve the two components, but obtained absorption spectra that were only $\sim 80\%$ saturated. The data quality and the judiciousness in setting the self-calibration parameters determine the reliability of an iterative self-calibration process. Lower data quality leads to longer, more elaborate calibrations which often require extensive flagging and ultimately challenge the soundness of the result. Starting with a self-calibration model that doesn't represent the known spatial distribution of flux only makes the process more unstable. Our data were taken in better conditions than the previous BIMA observations and with new SIS receivers, both of which contributing to a higher overall data quality. There were also different A-array antenna stations producing a better beam from which this image based reduction may have benefited. The calibration process involved only two iterations and varying the self-calibration parameters, such as the calibration interval and convergence criteria, produced consistent results. All of these considerations give us much confidence in the robustness of our result.

The residual flux in the absorption trough is thought to be due to small scale structure in the absorbing cloud which translates into a varying covering factor as a function of velocity (Wiklind & Combes 1998; Wiklind & Combes 1996; Frye et al. 1996). The asymmetry seen in the lines is also evidence of a complex, inhomogeneous absorbing medium. However, in order to get any quantitative information out of these profiles it is necessary to make simplifying assumptions about the equilibrium state of the gas and the structure.

The deep absorption prevents a direct determination of the physical parameters of the absorbing medium, however limits can be determined using a lower limit of the velocity integrated optical depth. The $HCO^+(2 \leftarrow 1)$ and $HCN(2 \leftarrow 1)$ line profiles presented here with their $(1 \leftarrow 0)$ counterparts presented in Menten et al. (1999) and Carilli et al. (1998) give low values for the rotation temperatures, $\lesssim 6\,\mathrm{K}$, consistent with previous analyses (Wiklind & Combes 1996; Menten et al. 1999). This result implies that HCN and HCO^+ are primarily excited by the CMB, so we can assume that the rotation temperature of these molecules are $T_{rot} \sim 5\,\mathrm{K}$ which is the temperature of the CMB at $z = 0.89$. This value of T_{rot} along with the calculated velocity integrated optical depths give lower limits to the column densities for HCN and HCO^+; $N(\mathrm{HCN}) \gtrsim 3 \times 10^{14}\mathrm{cm}^{-2}$ and $N(\mathrm{HCO}^+) \gtrsim 2 \times 10^{14}\,\mathrm{cm}^{-2}$.

The lensing galaxy in which this absorption is taking place is likely a massive, early-type spiral (Wiklind & Combes 1998; Wiklind & Combes 1996). Given that the abundance ratios are somewhat similar to the Milky Way, the column densities derived above imply an H_2 column of $N(H_2) \gtrsim 10^{22}$ but the low average excitation temperatures of the HCN and HCO^+ lines imply a moderately low average volume density ($\lesssim 10^4 \mathrm{cm}^{-3}$). Therefore the pathlength through the cloud must be greater than 1 pc, but it is not clear how extended the cloud is in the line of sight direction. The full velocity range over which there is absorption is $> 60\,\mathrm{km\,s^{-1}}$ which is not atypical for observations in the Milky Way (Frye et al. 1996). However according to galactic (Wiklind & Combes 1998) and lensing (Nair et al. 1993; Kochanek & Narayan 1992) models, the lensing galaxy of PKS 1830-211 is oriented almost face on ($i \simeq 16°$) and the light from the SW image is traversing the lensing galaxy at a galactocentric distance between 1.8 kpc and 3 kpc. Assuming this orientation, it is hard to imagine how the absorption occurs over such a large velocity range (see Menten et al. 1999).

5. Summary

The two main components of the gravitational lens PKS 1830-211 have been resolved with the BIMA interferometer. The continuum levels are $1.13 \pm 0.1\,\mathrm{Jy\,beam^{-1}}$ for the NE component and $0.96 \pm 0.1\,\mathrm{Jy\,beam^{-1}}$ for the SW component giving a flux ratio of 1.18 ± 0.06. These levels are expected to vary, but are consistent with other published values.

High-resolution spectra ($1.2\,\mathrm{km\,s^{-1}}$) of the redshifted lines of $HCO^+(2 \leftarrow 1)$ and HCN($2 \leftarrow 1$) were shown to reach the zero flux level in the SW image but with a non zero flux level averaged across the narrow trough. These results are an improvement over the previous BIMA observations of this object (Frye et al. 1996) and are in agreement with what would be expected from saturated absorption by a complex absorbing cloud with multiple components and small scale structure.

Comparing our line profiles with previously published spectra of the $HCO^+(1 \leftarrow 0)$ and HCN($1 \leftarrow 0$) transitions in the SW component (Menten et al. 1999; Carilli et al. 1998) gives a low upper bound on the excitation temperature, $\lesssim 6$ K, which translates to fairly high column densities, $N(\mathrm{HCN}) \gtrsim 3 \times 10^{14}\,\mathrm{cm^{-2}}$ and $N(HCO^+) \gtrsim 2 \times 10^{14}\,\mathrm{cm^{-2}}$. The high column densities imply a large H_2 column but the low excitation temperatures suggests that the volume density of H_2 is moderately low. Given the estimated galactocentric distance of the absorbing cloud ≥ 1.8 kpc and the inclination angle of the galaxy, $i \simeq 16°$, the line widths are remarkably large.

We would like to thank Dick Plambeck for helping with the many questions that arose during this research. Also thanks to Mel Wright for help with generating model observations and for general advice. Michiel Hogerheijde and Geoff Marcy both made helpful contributions. BLF would like to thank Joe Silk and Tom Broadhurst for their ideas and contributions. This research has been funded by NSF grant AST-9981308.

REFERENCES

[Carilli et al. 1998]Carilli, C., Menten, K., Reid, M., Rupen, M., & Claussen, M., 1998, in ASP Conf. Ser. 144, Radio Emission from Galactic and Extragalactic Compact Sources, ed. J. A. Zensus, G. B. Taylor, & J. M. Worbel (San Francisco: ASP), 317

[Engargiola & Plambeck 1998]Engargiola, G. & Plambeck, R., 1998, Proc. SPIE, 3357, 508

[Frye et al. 1996]Frye, B., Welch, W. J., & Broadhurst, T., 1996, ApJ, 478, L25

[Jauncey et al. 1991]Jauncey, D.L., et al. 1991, Nature, 352, 132

[Johns et al. 1996]Johns, D., et al. 1996, ApJ, 470, L23

[Kochanek & Narayan 1992]Kochanek C. & Narayan, R., 1992, ApJ, 401, 461

[Lidman et al. 1998]Lidman, C., Courbin, F., Meylan, G., Broadhurst, T., Frye, B., & Welch, W., 1998, ApJ, 524, L57

[Lovell et al. 1998]Lovell, J., Jauncey, D., Reynolds, J., Wieringa, M., King, E., Tzioumis, A., McCulloch, P., & Edwards, P., 1998, ApJ, 508, L51

[Menten et al. 1999]Menten, K., Carilli, C., & Reid, M., in ASP Conf. Ser. 156, Highly Redshifted Radio Lines, ed. C. L. Carilli, S. J. E. Radford, K. M. Menten, & G. I. Langston (San Francisco: ASP), 218

[Nair et al. 1993]Nair, S., Narashima, D., & Rao, P., ApJ, 407, 46

[Rao & Subrahmanyan 1988]Rao, P. & Subrahmanyan, R., 1988, MNRAS, 231, 229

[Subrahmanyan et al. 1990]Subrahmanyan, R., Narashima, D., Rao, A., & Swarup, G., 1990, MNRAS, 246, 263

[van Ommen et al. 1995]van Ommen, T., Jones, D., Preston, R., & Jauncey, D., ApJ, 444, 561.

[Welch et al. 1996]Welch, W., et al. 1996, PASP, 108, 93

[Wiklind & Combes 1996]Wiklind, T. & Combes, F., 1996, Nature, 379, 139

[Wiklind & Combes 1998]Wiklind, T. & Combes, F., 1998, ApJ, 500, 129

Fig. 1.— Upper sideband continuum map with the spectra from the NE and SW components overlayed. The contour levels are 10, 20, 30, 40, 50, 60, 70, 80, and 90%.

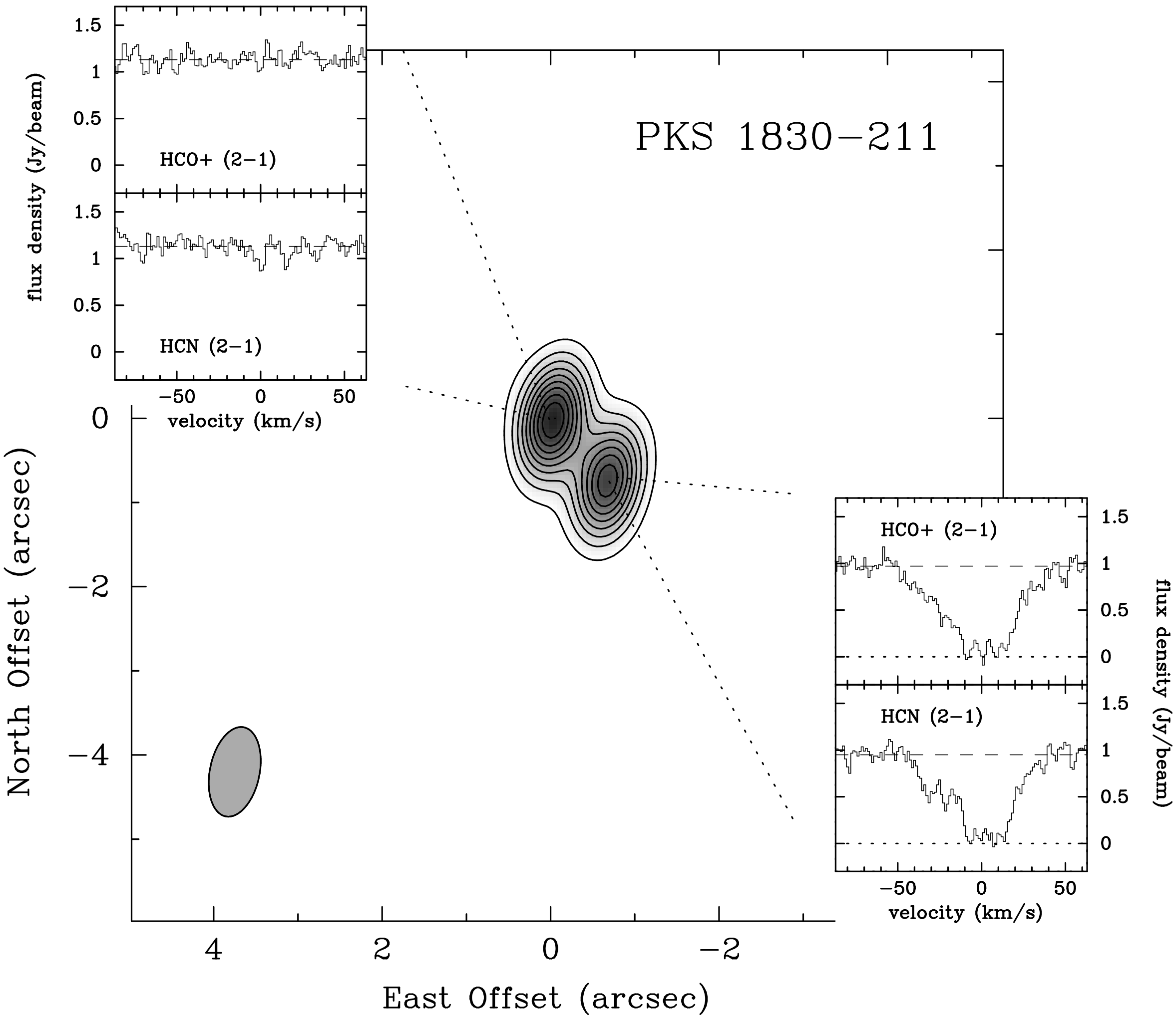
PKS 1830−211
HCO+ (2−1)
HCN (2−1)
flux density (Jy/beam)
velocity (km/s)
North Offset (arcsec)
East Offset (arcsec)